Abdelbary NH, Abdullah HM, Matsuzaki T, Hayashi D, Tanaka Y, Takashima H, **Izumo S, Kubota R.**	Reduced Tim-3 expression on human T-lymphotropic virus type I (HTLV-I) Tax-specific cytotoxic T lymphocytes in HTLV-I infection.	J Infect Dis.	203	948-959	2011
Kawabata T, Higashimoto I, Takashima H, **Izumo S, Kubota R**	Human T-lymphotropic virus type I (HTLV-I)-specific CD8+ cells accumulate in the lungs of patients infected with HTLV-I with pulmonary involvement.	J Med Virol.	84(7)	1120-1127	2012
Ando H, Sato T, Tomaru U, Yoshida M, Utsunomiya A, Yamauchi J, Araya N, Yagishita N, Coler-Reilly A, Shimizu Y, Yudoh K, Hasegawa Y, Nishioka K, Nakajima T, Jacobson S, **Yamano Y.**	Positive feedback loop via astrocytes causes chronic inflammation in virus-associated myelopathy.	Brain	136(9)	2876-2887	2013
Sato T, Coler-Reilly A, Utsunomiya A, Araya N, Yagishita N, Ando H, Yamauchi J, Inoue E, Ueno T, Hasegawa Y, Nishioka K, Nakajima T, Jacobson S, Izumo S, **Yamano Y.**	CSF CXCL10, CXCL9, and Neopterin as Candidate Prognostic Biomarkers for HTLV-1-Associated Myelopathy/Tropical Spastic Paraparesis.	PLoS Negl Trop Dis.	7(10)	e2479	2013
Sato T, Araya N, Yagishita N, Ando H, **Yamano Y.**	Host Immune System Abnormalities Among Patients with Human T-Lymphotropic Virus Type 1 (HTLV-1)-Associated Disorders.	T-Cell Leukemia,		65-80/234,	2011

Araya N, Takahashi K, Sato T, Nakamura T, Sawa C, Hasegawa D, Ando H, Aratani S, Yagishita N, Fujii R, Oka H, Nishioka K, Nakajima T, Mori N, **Yamano Y.**	Fucoidan therapy decreases the proviral load in patients with human T-lymphotropic virus type1-associated neurological disease.	Antivir Ther	16(1)	89-98	2011
Sone J, Kitagawa N, Sugawara E, Iguchi M, Nakamura R, Koike H, Iwasaki Y, Yoshida M, Takahashi T, Chiba S, Katsuno M, **Tanaka F,** Sobue G.	Neuronal intranuclear inclusion disease cases with leukoencephalopathy diagnosed via skin biopsy.	J Neurol Neurosurg Psychiatry.	85(3)	354-6.	2014
Iida A, Takahashi A, Kubo M, Saito S, Hosono N, Ohnishi Y, Kiyotani K, Mushiroda T, Nakajima M, Ozaki K, Tanaka T, Tsunoda T, Oshima S, Sano M, Kamei T, Tokuda T, Aoki M, Hasegawa K, Mizoguchi K, Morita M, Takahashi Y, Katsuno M, Atsuta N, Watanabe H, **Tanaka F**, Kaji R, Nakano I, Kamatani N, Tsuji S, Sobue G, Nakamura Y, Ikegawa S	A functional variant in ZNF512B is associated with susceptibility to amyotrophic lateral sclerosis in Japanese	Hum Mol Genet	20(18)	3684-3692	2011
Satoshi Nozuma , **Eiji Matsuura**, Toshio Matsuzaki, Osamu Watanabe, Ryuji Kubota, Shuji Izumo, Hiroshi Takashima.	Familial clusters of HTLV-1-associated myelopathy / tropical spastic paraparesis.	PLOS ONE	9(5)	doi: 10.1371/journal.pone.0086144.	2014

Saito M, Tanaka R, Arishima S, Matsuzaki T, Ishihara S, Tokashiki T, Ohya Y, Takashima H, Umehara F, Izumo S, Tanaka Y.	Increased expression of OX40 is associated with progressive disease in patients with HTLV-1-associated myelopathy/tropical spastic paraparesis.	Retrovirology.	10	51	2013
Kodama A, Tanaka R, **Saito M**, Ansari AA, Tanaka Y.	A novel and simple method for generation of human dendritic cells from unfractionated peripheral blood mononuclear cells within 2 days: its application for induction of HIV-1-reactive CD4 (+) T cells in the hu-PBL SCID mice.	Front Microbiol.	4	292	2013
Tanaka Y, Takahashi Y, Tanaka R, Kodama A, Fujii H, Hasegawa A, Kannagi M, Ansari AA, **Saito M.**	Elimination of human T cell leukemia virus type-1-infected cells by neutralizing and antibody-dependent cellular cytotoxicity-inducing antibodies against human T cell leukemia virus type-1 envelope gp46.	AIDS Res Hum Retroviruses.		in press	2014
Saito M	Pathogenic conversion of Foxp3+ T cells into Th17 cells: is this also the case for multiple sclerosis?	Clin Exp Neuroimmunol.		in press	2014

Ⅳ. 研究成果の刊行物・別刷

Journal of the Peripheral Nervous System 18:89–93 (2013)

CASE REPORT

Novel mutation in the replication focus targeting sequence domain of *DNMT1* causes hereditary sensory and autonomic neuropathy IE

Junhui Yuan[1], Yujiro Higuchi[1], Tatsui Nagado[2], Satoshi Nozuma[1], Tomonori Nakamura[1], Eiji Matsuura[1], Akihiro Hashiguchi[1], Yusuke Sakiyama[1], Akiko Yoshimura[1], and Hiroshi Takashima[1]

[1] *Department of Neurology and Geriatrics, Kagoshima University, Graduate School of Medical and Dental Sciences; and* [2] *Department of Neurology, Imakiire General Hospital, Kagoshima, Japan*

Abstract *DNMT1*, encoding DNA methyltransferase 1 (Dnmt1), is a critical enzyme which is mainly responsible for conversion of unmethylated DNA into hemimethylated DNA. To date, two phenotypes produced by *DNMT1* mutations have been reported, including hereditary sensory and autonomic neuropathy (HSAN) type IE with mutations in exon 20, and autosomal dominant cerebellar ataxia, deafness, and narcolepsy caused by mutations in exon 21. We report a sporadic case in a Japanese patient with loss of pain and vibration sense, chronic osteomyelitis, autonomic system dysfunctions, hearing loss, and mild dementia, but without definite cerebellar ataxia. Electrophysiological studies revealed absent sensory nerve action potential with nearly normal motor nerve conduction studies. Brain magnetic resonance imaging revealed mild diffuse cerebral and cerebellar atrophy. Using a next-generation sequencing system, 16 candidate genes were analyzed and a novel missense mutation, c.1706A>G (p.His569Arg), was identified in exon 21 of *DNMT1*. Our findings suggest that mutation in exon 21 of *DNMT1* may also produce a HSAN phenotype. Because all reported mutations of *DNMT1* are concentrated in exons 20 and 21, which encode the replication focus targeting sequence (RFTS) domain of Dnmt1, the RFTS domain could be a mutation hot spot.

Key words: DNA methyltransferase 1, *DNMT1*, hereditary sensory and autonomic neuropathy, missense mutation, next-generation sequencing

Introduction

DNA methyltransferase 1 (Dnmt1), encoded by *DNMT1*, is the principal enzyme responsible for the maintenance of cytosine methylation at cytosine–phosphate–guanine dinucleotides in the mammalian genome *(Feng and Fan, 2009)*, and is also crucial for gene regulation and chromatin stability *(Tohgi et al., 1999; Chen et al., 2003)*. Human Dnmt1 consists of a conserved C-terminal catalytic core and a large N-terminal region harboring multiple globular conserved domains, including the DNA methyltransferase-associated protein 1-binding domain, the proliferating cell nuclear antigen-binding domain, the replication focus targeting sequence (RFTS) domain, the CXXC domain, and two bromo-adjacent homology domains *(Syeda et al., 2011)*.

To date, eight kindreds with *DNMT1* mutations have been reported, half of which were characterized

Address correspondence to: Prof. Hiroshi Takashima, Department of Neurology and Geriatrics, Kagoshima University, Graduate School of Medical and Dental Sciences, 8-35-1 Sakuragaoka, Kagoshima City, Kagoshima 890-8520, Japan. Tel: +(81)99-275-5330; Fax: +(81)99-265-7164; E-mail: thiroshi@m3.kufm.kagoshima-u.ac.jp

© 2013 Peripheral Nerve Society

by sensory neuropathy, sensorineural hearing loss, and dementia, caused by mutations in exon 20 *(Klein et al., 2011)*; the other half presented with autosomal dominant cerebellar ataxia, deafness, and narcolepsy, and all mutations were located in exon 21 *(Winkelmann et al., 2012)*. It is noteworthy that all peptides coded by exon 20 and 21 belong to the RFTS domain of Dnmt1.

Using a next-generation sequencing (NGS) system, we screened a panel of candidate genes in a Japanese patient with sensory neuropathy, autonomic nervous system dysfunctions, sensorineural hearing loss, and slight dementia. This screen identified a novel missense mutation in exon 21 of *DNMT1*. We also reviewed all reported cases with *DNMT1* mutation and investigated the pathogenesis of various *DNMT1*-related phenotypes.

Case Report

The patient was a 41-year-old Japanese male from a non-consanguineous family (Fig. 1A). No neurological disorders were found in other family members. Pain perception began to decrease in his distal lower limbs after high school, and this condition progressed slowly. At the age of 30 and 32, after local infection, he had osteomyelitis in his first right toe and fifth left toe, respectively, and amputations were performed. Meanwhile, he began to experience hearing loss, and a hearing aid was used in the right ear. After his gait became unsteady he was referred to a department of neurology. Physical examination revealed foot ulcers and mutilations (Fig. 1B). His muscle strength was normal; however, a marked decrease was observed in his sense of pain and touch (1/10) in the lower limbs. Vibration perception was present in the fingers but absent in the lower limbs, and Romberg test was positive. Mild mental retardation was noted. Examination of the cranial nerves was normal except for bilateral hearing loss. Cerebellar function examination showed no abnormalities on finger-to-nose or heel-to-knee testing, or rapidly alternating pronation and supination of hands. Muscle tone was normal, without speech abnormality. The deep tendon reflexes of the lower limbs were absent. The pure tone audiometry test suggested moderate to severe bilateral sensorineural hearing loss. A 24-h Holter monitor indicated sinus bradycardia (43/min on average). Plain radiographs showed an amputation stump of the right hallux and left little toe, accompanied by bone destruction, cortical bone thickness or sclerosis, and an irregular articular surface (Figs. 1C and 1D). Brain magnetic resonance imaging (MRI) revealed mild diffuse cerebral and cerebellar atrophy (Fig. 1E). Clinical and radiological examinations revealed several saprodontia, bronchiectasis in the middle and lower lobe of the right lung, and accessory sinusitis.

In the electrophysiological study, except for the slight slowing of motor nerve conduction velocity in the right tibial nerve, motor nerve conduction studies were almost normal in the median, ulnar, and posterior tibial nerves. However, the sensory nerve action potential could not be evoked in the right median, ulnar, and sural nerves.

The protocol of the studies described below was reviewed and approved by the Institutional Review Board of Kagoshima University. The patient provided his written informed consent to participate in this study.

Methods and Results

Sixteen candidate genes, including 11 genes related to hereditary sensory and autonomic neuropathies (HSAN) and another 5 genes (Table 1) associated with sensory and autonomic dysfunctions were screened on the MiSeq sequencing system Illumina, San Diego, CA, USA).

After one run for 28 h, 400,122 (150 × 2) reads were generated for this patient on the NGS; 93.7% of the reads could be mapped to the reference genome and 98.1% of the target regions were covered at least 10 times. In 27 high-confidence variants, 24 known single nucleotide polymorphisms (SNPs) were coincident with the dbSNP (http://www.ncbi.nlm.nih.gov/snp/) or 1000 Genomes data (http://browser.1000genomes.org). Of the remaining three non-synonymous variants, c.3248A>C in *KIF1A* and c.3448T>C in *SCN9A* were also found in the normal control, and were thus considered SNPs. Besides, a heterozygous missense mutation, c.1706A>G (p.His569Arg) in exon 21 of the *DNMT1* gene (NM_001130823.1, NP_001124295.1) remained and was confirmed by Sanger sequencing (Figs. 2A and 2B). This mutation is located in a highly conserved domain among different species (Fig. 2C). Using the web-based programs, this His569Arg alteration was predicted to be pathogenic in POLYPHEN2 (0.982) and SIFT (0.00).

This mutation was not observed in 100 Japanese control samples, nor did we find it on the 1000 Genomes web site, which catalogs human genetic variations using 2,500 samples, including 500 East Asian (100 Japanese) samples.

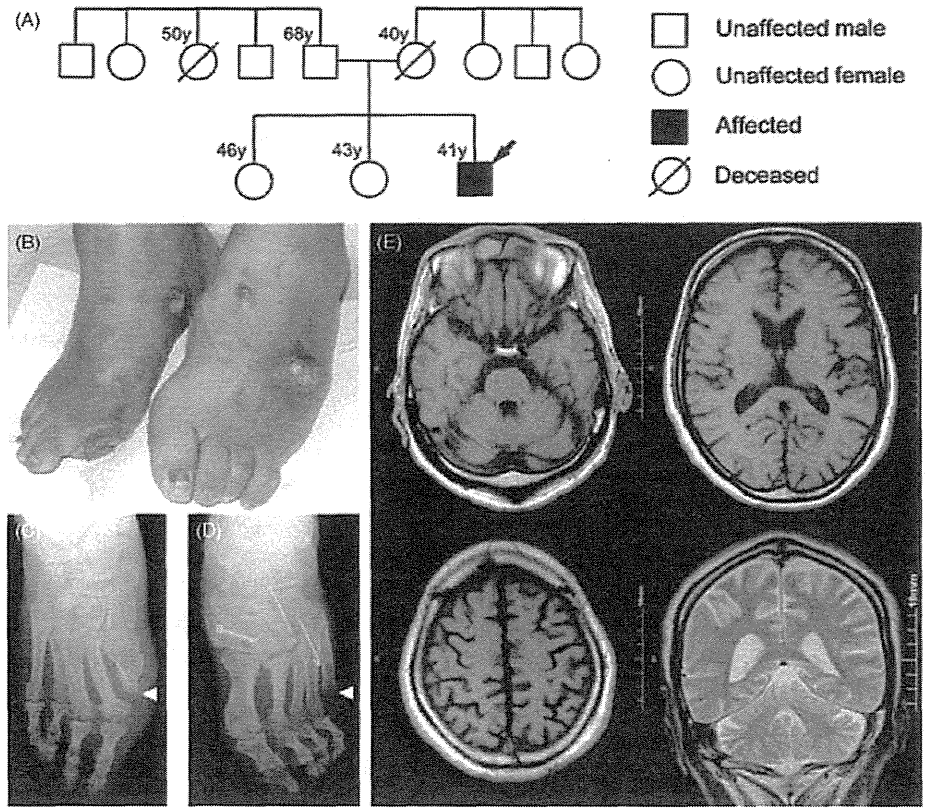

Figure 1. Pedigree and clinical photographs. (A) Pedigree of the patient. The arrow (→) indicates the index case. (B) Foot ulcers and mutilations. (C, D) Radiographs showing the amputation stump of the right hallux and left little toe (◻) accompanied by chronic osteomyelitis. (E) Brain magnetic resonance imaging showing mild and diffuse cerebral and cerebellar atrophy.

Table 1. Candidate genes screened using Miseq sequencing system.

Gene symbol	Locus	Coding exons	Reference sequences
SPTLC1	9q22.31	15	ENST00000262554
SPTLC2	14q24.3	12	ENST00000216484
ATL1	14q11	14	ENST00000441560
DNMT1	19p13.2	41	ENST00000359526
WNK1	12p13.33	28	ENST00000537687
FAM134B	5p15.1	9	ENST00000306320
KIF1A	2q37.3	49	ENST00000498729
IKBKAP	9q31.3	37	ENST00000374647
NTRK1	1q23.1	16	ENST00000368196
NGF	1p13.2	3	ENST00000369512
DST	6p12.1	84	ENST00000244364
SCN9A	2q24.3	27	ENST00000303354
CCT5	5p15.2	11	ENST00000280326
PRNP	20p13	2	ENST00000379440
FLVCR1	1q32.3	10	ENST00000366971
RNF170	8p11.21	7	ENST00000527424

Discussion

We report a Japanese patient with suspected HSAN. Using a high-throughput NGS system, we established a diagnostic procedure involving screening of 16 candidate genes in one run, and identified a novel missense mutation in exon 21 of *DNMT1*.

In 2011, *DNMT1*-related dementia, deafness, and sensory neuropathy was demonstrated in four kindreds from America, Europe, and Japan and was designated HSAN IE. It is an autosomal dominant degenerative disorder of the central and peripheral nervous systems characterized by sensory impairment, sudomotor dysfunction (loss of sweating), dementia, and sensorineural hearing loss. Affected individuals are normal in their youth but begin to manifest progressive sensorineural deafness and sensory neuropathy by the age of 20–35 *(Klein et al., 2011)*. In 2012, another four kindreds from Europe were found to have early onset (18–44 years) of a narcolepsy/cataplexy syndrome followed by ataxia, deafness, sensory neuropathy, and memory loss, which was reported to be associated with *DNMT1* mutations *(Winkelmann et al., 2012)*.

The present patient was normal until graduation from senior high school, but began to manifest progressive inability to perceive pain and experienced painless osteomyelitis. Deafness, as the second symptom, started after the age of 30, and an examination

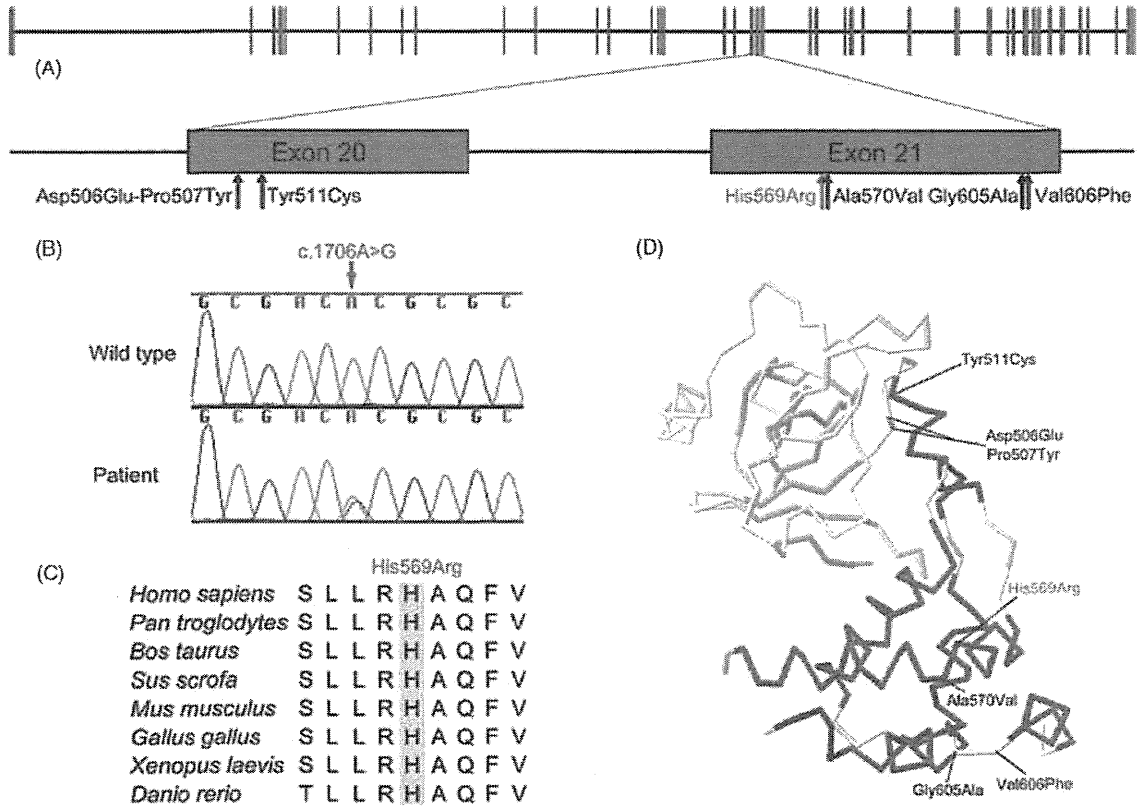

Figure 2. Genetic studies and mutations review. (A) Schematic overview and all mutations in exons 20 and 21 of *DNMT1*. (B) Sequencing chromatogram of the c.1706A>G mutation. Red arrow indicates the mutation site in present patient. (C) Amino acid sequence at the mutation site in homologs of DNA methyltransferase 1 aligned by CLUSTALW. A yellow bar indicates the highly conserved histidine at position 569. (D) Location of mutated residues in the crystal structure of the replication focus targeting sequence domain (Protein Data Bank accession number 3EPZ, showing residues 367–616 in NP_001124295.1).

revealed bilateral sensorineural hearing loss. His gait became ataxic and there was no vibration perception in the lower limbs. Although cerebellar atrophy was revealed by the brain MRI, no definite cerebellar dysfunction was identified. After examination, his ataxia was considered mainly due to loss of deep sensation. The electrophysiological studies revealed sensory dominant axonal polyneuropathy. In addition, mental retardation was observed by the neurologist and diffuse cerebral and cerebellar atrophy was noted in the brain MRI. All these findings were consistent with HSAN IE. The patient's sinus bradycardia and other dysfunctions of the respiratory system might have resulted from the autonomic nervous system dysfunction, but no reliable test was performed to check his autonomic nervous function.

Using the MiSeq sequencing system, a heterozygous missense mutation, c.1706A>G (p.His569Arg), was identified in exon 21 of *DNMT1*. As the present patient showed a definite HSAN phenotype, our findings indicated that the variable *DNMT1*-related phenotype was unlikely to have been determined by the location of the mutation. Although no narcolepsy/cataplexy was noted either in our case or the original four kindreds, the mechanism underlying the varied phenotypes requires further investigation.

It is noteworthy that all reported mutations of *DNMT1* were located in exon 20 (*Klein et al., 2011*: p.Asp506Glu-Pro507Tyr, p.Tyr511Cys; NP_001124295.1) and exon 21 (*Winkelmann et al., 2012*: p.Ala570Val, p.Gly605Ala, p.Val606Phe; NP_001124295.1), and that the original presentations were sensory neuropathy and narcolepsy/cataplexy syndrome, respectively. In Dnmt1, all the peptides encoded by exons 20 and 21 belong to the RFTS domain (Fig. 2D). Previous research indicated that this RFTS domain, inserted deeply into the DNA-binding pocket *(Takeshita et al., 2011)*, contributes to the inhibition of Dnmt1 binding to naked DNA oligonucleotides and native polynucleosomes *(Syeda et al., 2011)*. The RFTS domain also contains a binding site for Uhrf1 *(Achour et al., 2008)*, which recognizes and binds to the hemimethylation sites of DNA and recruits Dnmt1 *(Bostick et al., 2007; Arita et al., 2008;*

Avvakumov et al., 2008). Mutations in exon 20 and 21 of *DNMT1* would transform the structure of the RFTS domain and affect the recognition and binding procedure of hemimethylated DNA, creating abnormal methylation and gene silencing. On the basis of our findings and previous studies, we surmise that the RFTS domain is a mutation hot spot compared with the other Dnmt1 domains. The other possibility is that mutation in other functional domains might cause global genome demethylation and embryonic lethality.

In conclusion, using a MiSeq sequencing system we identified a novel missense mutation in exon 21 of *DNMT1* in a Japanese patient with the typical HSAN IE phenotype. We also reviewed all eight of the kindreds with *DNMT1* mutations in previous reports, and excluded the presumption that varied phenotypes were generated by mutations in different exons. However, further research is required to elucidate the mechanisms of alterations in the RFTS domain and their influence on the DNA methylation procedure.

Acknowledgements

The authors thank Ms. A. Nishibeppu of our department for her excellent technical assistance. The authors would like to thank Enago (www.enago.jp) for the English language review. The authors thank the Joint Research Laboratory, Kagoshima University Graduate School of Medical and Dental Sciences for the use of their facilities. The study was funded by the research on the Nervous and Mental Disorders and Research Committee for Charcot-Marie-Tooth Disease, Neuropathy, Ataxic Disease and Applying Health and Technology of Ministry of Health, Welfare and Labour, Japan.

References

Achour M, Jacq X, Rondé P, Alhosin M, Charlot C, Chataigneau T, Jeanblanc M, Macaluso M, Giordano A, Hughes AD, Schini-Kerth VB, Bronner C (2008). The interaction of the SRA domain of ICBP90 with a novel domain of DNMT1 is involved in the regulation of VEGF gene expression. Oncogene 27:2187–2197.

Arita K, Ariyoshi M, Tochio H, Nakamura Y, Shirakawa M (2008). Recognition of hemi-methylated DNA by the SRA protein UHRF1 by a base-flipping mechanism. Nature 455:818–821.

Avvakumov GV, Walker JR, Xue S, Li Y, Duan S, Bronner C, Arrowsmith CH, Dhe-Paganon S (2008). Structural basis for recognition of hemi-methylated DNA by the SRA domain of human UHRF1. Nature 455:822–825.

Bostick M, Kim JK, Estève PO, Clark A, Pradhan S, Jacobsen SE (2007). UHRF1 plays a role in maintaining DNA methylation in mammalian cells. Science 317:1760–1764.

Chen WG, Chang Q, Lin Y, Meissner A, West AE, Griffith EC, Jaenisch R, Greenberg ME (2003). Derepression of BDNF transcription involves calcium-dependent phosphorylation of MeCP2. Science 302:885–889.

Feng J, Fan G (2009). The role of DNA methylation in the central nervous system and neuropsychiatric disorders. Int Rev Neurobiol 89:67–84.

Klein CJ, Botuyan MV, Wu Y, Ward CJ, Nicholson GA, Hammans S, Hojo K, Yamanishi H, Karpf AR, Wallace DC, Simon M, Lander C, Boardman LA, Cunningham JM, Smith GE, Litchy WJ, Boes B, Atkinson EJ, Middha SB, Dyck PJ, Parisi JE, Mer G, Smith DI, Dyck PJ (2011). Mutations in DNMT1 cause hereditary sensory neuropathy with dementia and hearing loss. Nat Genet 43:595–600.

Syeda F, Fagan RL, Wean M, Avvakumov GV, Walker JR, Xue S, Dhe-Paganon S, Brenner C (2011). The replication focus targeting sequence (RFTS) domain is a DNA-competitive inhibitor of Dnmt1. J Biol Chem 286:15344–15351.

Takeshita K, Suetake I, Yamashita E, Suga M, Narita H, Nakagawa A, Tajima S (2011). Structural insight into maintenance methylation by mouse DNA methyltransferase 1 (Dnmt1). Proc Natl Acad Sci U S A 108:9055–9059.

Tohgi H, Utsugisawa K, Nagane Y, Yoshimura M, Genda Y, Ukitsu M (1999). Reduction with age in methylcytosine in the promoter region −224 approximately −101 of the amyloid precursor protein gene in autopsy human cortex. Brain Res Mol Brain Res 70:288–292.

Winkelmann J, Lin L, Schormair B, Kornum BR, Faraco J, Plazzi G, Melberg A, Cornelio F, Urban AE, Pizza F, Poli F, Grubert F, Wieland T, Graf E, Hallmayer J, Strom TM, Mignot E (2012). Mutations in DNMT1 cause autosomal dominant cerebellar ataxia, deafness and narcolepsy. Hum Mol Genet 21:2205–2210.

Hereditary sensory and autonomic neuropathy type IID caused by an *SCN9A* mutation

Junhui Yuan, MD
Eiji Matsuura, MD, PhD
Yujiro Higuchi, MD
Akihiro Hashiguchi, MD
Tomonori Nakamura, MD, PhD
Satoshi Nozuma, MD
Yusuke Sakiyama, MD, PhD
Akiko Yoshimura, BS
Shuji Izumo, MD
Hiroshi Takashima, MD, PhD

Correspondence to Dr. Takashima: thiroshi@m3.kufm.kagoshima-u.ac.jp

ABSTRACT

Objective: To identify the clinical features of Japanese patients with suspected hereditary sensory and autonomic neuropathy (HSAN) on the basis of genetic diagnoses.

Methods: On the basis of clinical, in vivo electrophysiologic, and pathologic findings, 9 Japanese patients with sensory and autonomic nervous dysfunctions were selected. Eleven known HSAN disease-causing genes and 5 related genes were screened using a next-generation sequencer.

Results: A homozygous mutation, c.3993delGinsTT, was identified in exon 22 of *SCN9A* from 2 patients/families. The clinical phenotype was characterized by adolescent or congenital onset with loss of pain and temperature sensation, autonomic nervous dysfunctions, hearing loss, and hyposmia. Subsequently, this mutation was discovered in one of patient 1's sisters, who also exhibited sensory and autonomic nervous system dysfunctions, with recurrent fractures being the most predominant feature. Nerve conduction studies revealed definite asymmetric sensory nerve involvement in patient 1. In addition, sural nerve pathologic findings showed loss of large myelinated fibers in patient 1, whereas the younger patient showed normal sural nerve pathology.

Conclusions: We identified a novel homozygous mutation in *SCN9A* from 2 Japanese families with autosomal recessive HSAN. This loss-of-function *SCN9A* mutation results in disturbances in the sensory, olfactory, and autonomic nervous systems. We propose that *SCN9A* mutation results in the new entity of HSAN type IID, with additional symptoms including hyposmia, hearing loss, bone dysplasia, and hypogeusia. ***Neurology*® 2013;80:1641–1649**

GLOSSARY

CIP = channelopathy-associated insensitivity to pain; **CMAP** = compound muscle action potentials; **HSAN** = hereditary sensory and autonomic neuropathy; **$Na_V1.7$** = voltage-gated sodium channel; **dbSNP** = single nucleotide polymorphism database; **SCV** = sensory nerve conduction velocity; ***SCN9A*** = sodium channel, voltage-gated, type 9, α; **SNAP** = sensory nerve action potentials.

Hereditary sensory and autonomic neuropathy (HSAN) is a clinically and genetically heterogeneous group of disorders. Until now, HSAN has been classified into 6 main groups on the basis of their mode of inheritance and clinical features, and 11 HSAN disease–causing genes have been identified (table 1[1–17]).

SCN9A encodes the voltage-gated sodium channel ($Na_V1.7$), and the gain-of-function mutations result in several painful disorders, including inherited erythromelalgia,[18] paroxysmal extreme pain disorder,[19] and small nerve fiber neuropathy.[20] Loss-of-function *SCN9A* mutations have been linked to channelopathy-associated insensitivity to pain (CIP), which is characterized by congenital insensitivity to pain perception and anosmia; however, the autonomic dysfunction has been regarded as exclusionary criteria for the diagnosis of CIP.[21] It is noteworthy that no definite abnormalities have been recorded using either nerve conduction studies or sural nerve pathologic examinations in all of the previous cases with homozygous loss-of-function *SCN9A* mutations and part with compound heterozygous mutations.[22–26] However, a slight reduction in sensory nerve action potentials (SNAP) was recorded in two cases with compound heterozygous *SCN9A* mutations.[25,27]

Supplemental data at www.neurology.org

From the Department of Neurology and Geriatrics (J.Y., E.M., Y.H., A.H., T.N., S.N., Y.S., A.Y., H.T.), Kagoshima University, Graduate School of Medical and Dental Sciences, Kagoshima; and Department of Molecular Pathology (S.I.), Center for Chronic Viral Diseases, Kagoshima University School of Medicine, Kagoshima, Japan.

Go to Neurology.org for full disclosures. Funding information and disclosures deemed relevant by the authors, if any, are provided at the end of the article.

© 2013 American Academy of Neurology

© 2013 American Academy of Neurology. Unauthorized reproduction of this article is prohibited.

Table 1 Overview of HSAN disease-causing genes, inheritance pattern, and cardinal phenotypic features

Gene symbol	HSAN type	Inh	Onset age	Cardinal clinical features
SPTLC1	IA	AD	Adulthood	Loss of pain and temperature sensation; occasional autonomic involvement; variable sensorineural deafness and distal motor involvement[1,2]
SPTLC2	IC	AD		
ATL1	ID	AD	Early adulthood	Severe loss of pain, temperature, and vibration sensation; ulcero-mutilation; spastic paraparesis; rare autonomic involvement[3]
DNMT1	IE	AD	Childhood–adulthood	Severe sensory loss; ulcero-mutilation; sensorineural hearing loss; early-onset dementia; no autonomic symptoms[4–6]
WNK1	IIA	AR	Congenital—early childhood	Severe distal loss of touch, pain, and temperature sensation; mutilations in hands and feet; mild or asymptomatic autonomic dysfunction[7,8]
FAM134B	IIB	AR	Childhood	Severe loss of pain and temperature sensation; ulcero-mutilation; autonomic dysfunctions[9]
KIF1A	IIC	AR	Childhood	Severe loss of pain, temperature, vibration, and position sensation; ulcero-mutilation; distal muscle weakness; developmental delay and short stature[10]
IKBKAP	III	AR	Congenital	Familial dysautonomia; gastrointestinal and respiratory dysfunction; scoliosis; relative indifference to pain and temperature[11–13]
NTRK1	IV	AR	Congenital—early childhood	Loss of pain and temperature sensation; anhidrosis; episodic fever; mild mental retardation; joint deformities[14]
NGF	V	AR	Congenital—adulthood	Reduced sensation of pain and temperature; variable autonomic dysfunctions; painless fractures; joint deformities; mild mental retardation[15,16]
DST	VI	AR	Congenital	Dysautonomia; hypotonia; facial deformity; decreased pain response; joint contractures; retardation; respiratory failure; early death[17]

Abbreviations: AD = autosomal dominant; AR = autosomal recessive; *ATL1* = atlastin GTPase 1; *DNMT1* = DNA (cytosine-5)-methyltransferase 1; *DST* = dystonin; *FAM134B* = family with sequence similarity 134, member B; *IKBKAP* = inhibitor of κ light polypeptide gene enhancer in B cells, kinase complex-associated protein; Inh = inheritance; *KIF1A* = kinesin family member 1A; *NGF* = nerve growth factor (β polypeptide); *NTRK1* = neurotrophic tyrosine kinase, receptor, type 1; *SPTLC1* = serine palmitoyltransferase, long chain base subunit 1; *SPTLC2* = serine palmitoyltransferase, long chain base subunit 2; *WNK1* = WNK lysine deficient protein kinase 1.

In this study, using a next-generation sequencer, in 9 Japanese patients who were diagnosed with HSAN based on their clinical, in vivo electrophysiologic, and pathologic features, 11 known HSAN disease–causing genes and 5 related genes including *SCN9A* were screened. We identified a homozygous frameshift mutation in *SCN9A* of 2 patients/families. Therefore, we demonstrate that loss-of-function *SCN9A* mutation can produce a typical HSAN phenotype, and we propose this new classification as HSAN type IID. This study also broadened the spectrum of clinical phenotypes in patients with *SCN9A*-related disorders. Furthermore, on the basis of clinical, in vivo electrophysiologic, and pathologic findings, we attempted to elucidate the pathogenesis of the mutated $Na_V1.7$.

METHODS All patients who were referred to our department from 2000 to 2012 and who had sensory and autonomic nerve dysfunctions were selected. After excluding patients who had associated multiple motor nerve involvement, 9 patients were enrolled and genotyped in this study. Besides the 11 known HSAN disease-causing genes described above, we also investigated another 5 genes that might also cause sensory and autonomic symptoms, including *SCN9A*, *CCT5*, *PRNP*, *FLVCR1*, and *RNF170*.

The protocol of the following study was reviewed and approved by the Institutional Review Board of Kagoshima University. All patients and family members provided written informed consent to participate in this study.

Pathologic study. Sural nerve biopsies, performed at the age of 42 years in patient 1 and at the age of 25 years in patient 2, were analyzed according to standard morphologic procedures for light and electron microscopy.[18] A portion of the specimen was prepared for teased fiber analysis and classified according to Dyck's criteria.[19] The diameter and density of the myelinated fibers were analyzed with a Luzex AP image analyzer (Nireco Corporation, Tokyo, Japan).

Mutation sequencing. Genomic DNA was extracted from the peripheral blood leukocytes.

Using the Primer 3 program, we designed 375 oligonucleotide primers that covered all 357 coding exons and exon-intron junctions with amplicon lengths of 400–500 base pairs. Briefly, all target fragments of 9 patients were amplified by multiplex PCR (QIAGEN Multiplex PCR Kit; QIAGEN GmbH, Hilden, Germany) and ligated with specified indexes, respectively, then screened on the MiSeq sequencing system simultaneously in

© 2013 American Academy of Neurology. Unauthorized reproduction of this article is prohibited.

accordance with the manufacturer's protocol. The results were mapped to the genome reference sequence in the CLC Genomics Workbench 4 (CLC Bio, Aarhus, Denmark) and then analyzed with tablet software.[30]

The polymorphic and pathogenic natures of the confirmed variants were checked against the single nucleotide polymorphism database (dbSNP) (http://www.ncbi.nlm.nih.gov/snp/) and the 1000 Genomes database (http://browser.1000genomes.org/index.html). To confirm the suspected pathogenic mutations or low coverage domains (depth less than 10) in the MiSeq sequencing output, Sanger sequencing was also performed using the same methodology as the one employed in a previous study.[31] We screened 100 Japanese population control patients for the c.3993delGinsTT mutation.

RESULTS **Patients.** ***Patient 1.*** This 50-year-old man was the sixth child from a consanguineous family. No abnormalities were noted at birth or in the early developmental stages except for slight hyposmia since childhood. Since primary school, pain perception started to decrease in his hands and feet. At 30 years of age, he underwent lumbar spinal fixation, but felt no pain. After 40 years of age, the numbness progressed from the distal to the proximal limbs. Furthermore, his toes could not perceive temperature well when he entered his bath, and while walking, his right slipper always slipped off. There was no history of episodes of unexplained vomiting or dysphagia. A detailed physical examination revealed multiple skin lesions, including a burn mark on the right middle finger, which was caused by a cigarette. No pupillary abnormalities were observed. His muscle strength was normal, except grade 4+/5 weakness in the right tibialis anterior muscle. He also had a slight steppage gait. All reflexes were diminished, and his pathologic reflexes were negative. Pain and temperature perception were reduced in the distal limbs and absent in his feet. However, sense of vibration, joint position, and pressure were all preserved. Postural hypotension was excluded. During the sweating test, no sweating was observed in his face or any of his limbs, except in the palm of his left hand. Asymptomatic sensorineural hearing loss with an increase in the 4,000-Hz threshold in the left ear was diagnosed by an otorhinolaryngologist. MRI of the brain was normal.

In nerve conduction study, all motor nerve conduction velocity and compound muscle action potentials (CMAP) values were normal, except for a slightly reduced CMAP in the right tibial nerve at 3.5 mV (normal range, >4.4 mV). Sensory nerve conduction velocity (SCV) was slightly slow in the right median and ulnar nerve at 45.2 m/s (normal range, >47.2 m/s) and 40 m/s (normal range, >46.9 m/s), respectively, and moderately slow in the right sural nerve at 27.5 m/s (normal range, >40.8 m/s). SNAP amplitudes were markedly reduced in the right median nerve (0.9 μV; normal range, >7.0 μV), bilateral ulnar nerves (1.3 and 2.2 μV; normal range, >6.9 μV), and the right sural nerves (1.0 μV; normal range, >5.0 μV). However, the SCV and SNAP in the left median nerve were normal.

Patient 2. This 33-year-old man was from a nonconsanguineous family having no history of neurologic

Figure 1 **Clinical pictures of patient 2**

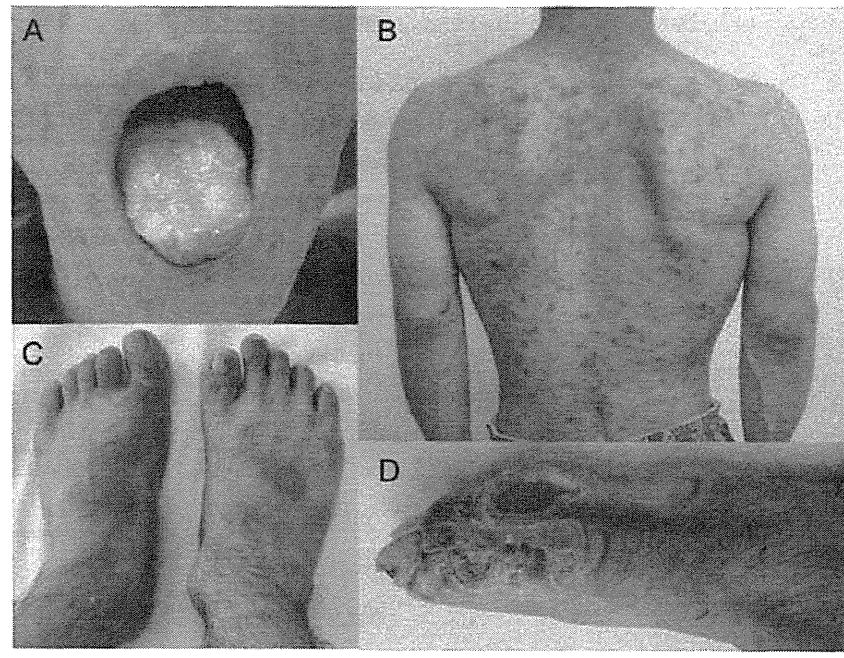

(A) Reduced number of fungiform papilla on the tongue. (B) The back of patient 2, showing scattered rash, pigmentation, and short humerus. (C) Short right hallux. (D) Multiple painless ulcers and deformed joints in the fingers.

© 2013 American Academy of Neurology. Unauthorized reproduction of this article is prohibited.

disorders. Decreased pain and temperature perception was noted at birth. When he was a year old, his feet were burnt after he walked on asphalt on a hot summer day, and this eventually progressed to osteomyelitis. Subsequently, he underwent operations of the right tibia and both feet, but he could not feel any pain. Before enrolling in primary school, hearing loss in the left ear and hyposmia were detected. He experienced occasional urinary and fecal incontinence, and frequent urination at night. His height was 157 cm, and he had a short humerus (27.5 cm) and right hallux (figure 1, B and C). Left acetabular dysplasia was noticed, which contributed to his left lower limb being 3 cm longer than his right lower limb. Rash and pigmentation were scattered over his chest and back (figure 1B), and several painless ulcers and deformed joints were observed in his fingers (figure 1D). Tendon hyperreflexia was noted in the lower limbs, and pathologic reflexes were negative. Pain perception was impaired in a glove–stocking pattern. Sense of vibration, joint position, and pressure were all normal. The sweating test revealed reduced sweating tendency throughout the body and especially in the trunk, except for his hands and feet. Postural hypotension was excluded, and brain MRI was normal. A lacrimal secretion anomaly was also detected. Otorhinolaryngologic examinations revealed the following: deafness in the left ear and minimal hearing loss in the right ear, glossopharyngeal and chorda tympani nerve abnormalities in the gustatory sensation test, reduced number of fungiform papilla on his tongue (figure 1A), and a decline in olfactory acuity as tested by a jet stream olfactometer. Examinations of the urinary tract excluded any organic disease.

The nerve conduction study revealed all motor nerve conduction velocity and CMAP values within normal ranges. The SCV was slightly slow in the right median and ulnar nerves (45.2 m/s and 46.2 m/s, respectively). However, SNAP was moderately decreased in the bilateral median (7 and 5.7 μV) and ulnar (3.3 and 4.4 μV) nerves. Nevertheless, no abnormalities were detected in sural nerve SCV and SNAP values.

Patient 3. This 55-year-old woman was an elder sister of patient 1. Her pregnancy was uneventful and delivery was normal. She had recurrent fractures and underwent operations for the left thigh (at age of 3 years and 8 years), right thigh (at age 11 years), and left elbow (primary school). When she was 30 years old, she perceived no pain after her feet were burnt on a heater. Anhidrosis was also noted, but after the age of 45 years, occasional sweat was secreted on her back. There was no evident hyposmia or hearing loss. At present, she is able to stand up and walk using

Figure 2 Clinical courses of the 3 patients

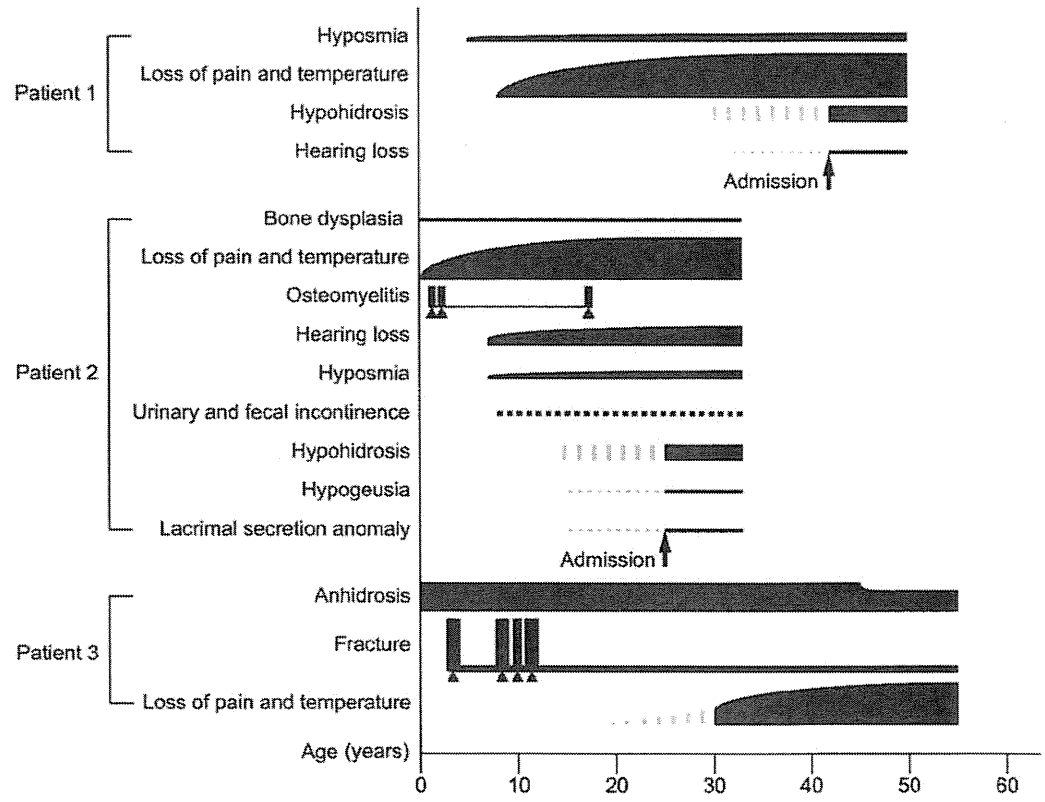

The solid triangles (▲) indicate surgery.

© 2013 American Academy of Neurology. Unauthorized reproduction of this article is prohibited.

her hands for support. Cranial nerve examinations were normal. Deformities of the left elbow, right foot, and bilateral lower limbs were noted. Muscle strength testing was normal in the upper limbs, whereas the strength in the lower limb muscles decreased to grades 2/5–4/5. Pain and temperature perceptions were reduced in the distal lower limbs and the anterior part of the right thigh, which may have been involved because of damage from surgery. The sense of vibration and joint position were preserved. Reflexes in her lower limbs were absent, and her pathologic reflexes were negative. Osteoporosis was excluded by an orthopedist.

The clinical courses of the 3 patients described above, including the onset and imaged severities of each symptom, are shown in figure 2.

Pathologic studies. In patient 1, the number of myelinated fibers was markedly decreased in all fasciculi, but the changes varied in their scale and extent. A histogram of the fiber diameter indicated a marked loss of large myelinated fibers relative to small myelinated fibers. Some remaining myelinated fibers had thinner myelin sheaths and some exhibited axonal degeneration. An electron microscopic study revealed clusters of Schwann cell processes, which may have been caused by the axonal degeneration of unmyelinated fibers (figure 3A). Contrary to the findings in patient 1, the number of myelinated fibers in patient 2 was slightly decreased, even with marked clinical symptoms. The histogram of fiber diameter showed a normal pattern. Electron microscopy showed that unmyelinated fibers were fairly preserved (figure 3B). No demyelinated fibers or inflammatory cells could be found in either patient.

Genetic studies. Using the MiSeq sequencing system, all of the 9 patients were genotyped successfully. Besides patients 1 and 2, no pathogenic mutation was detected. The CLCbio software showed that 96.24% and 93.6% of the data matched the reference sequences in patients 1 and 2, respectively. In the 357 targeted exons, 98.04% and 97.76% covered more than 10 reads. From patients 1 and 2, a total of 41 high-confidence variants were detected (table e-1 on the *Neurology*® Web site at www.neurology.org). In these variants, 39 known SNPs were coincident with the dbSNP or 1000 Genome database. Of the remaining 2 variants, the c.3248A>C in *KIF1A* was found in normal controls and was therefore considered as an SNP. A homozygous mutation in exon 22 of *SCN9A*, c. 3993delGinsTT, remained. This mutation was not observed in 100 Japanese control patient samples,

Figure 3 Pathologic findings from the sural nerve biopsies

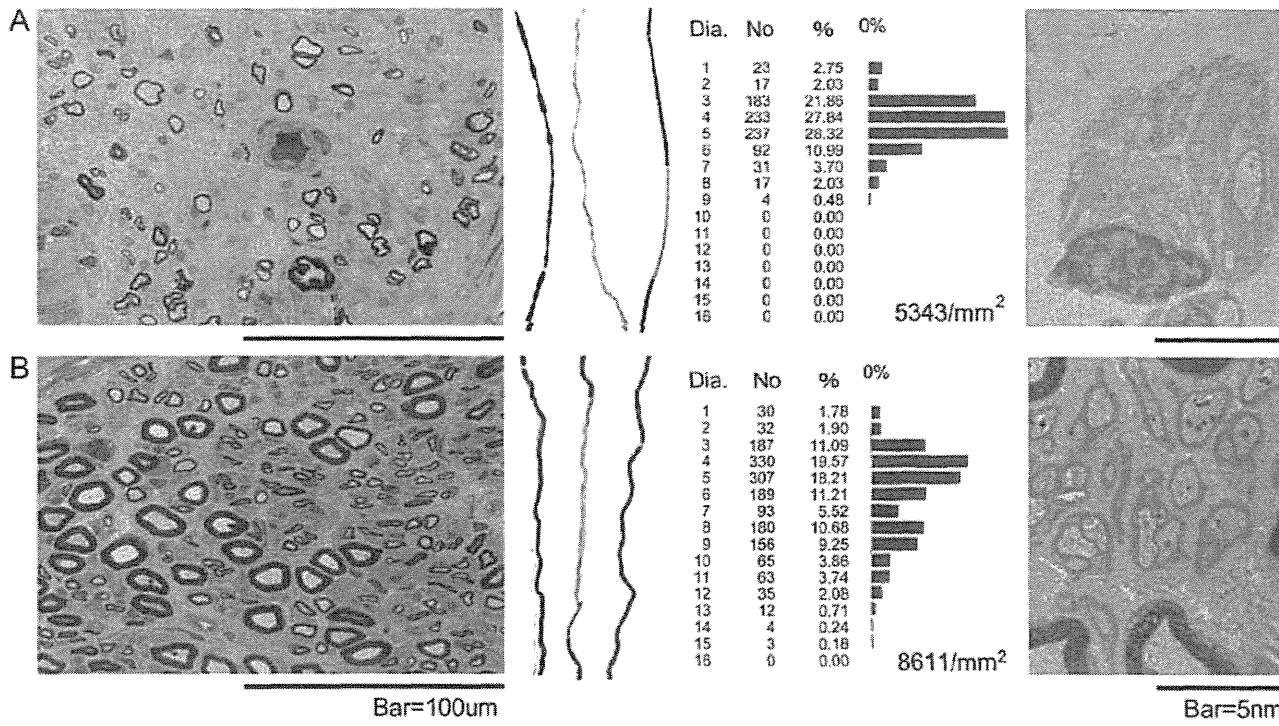

In patient 1, the density of large and small myelinated fibers is markedly decreased. The remaining myelinated fibers have thinner myelin sheaths. Some teased fibers exhibit axonal degeneration. The histogram of the fiber diameter indicates loss of large myelinated fibers (5,343 fibers/mm²). Electron microscopic examination shows clusters of Schwann cell processes (A). In patient 2, the densities of large and small myelinated fibers are slightly decreased. Teased fibers exhibit shortened internodal remyelination. The histogram of the fiber diameter shows a normal pattern (8,611 fibers/mm²). Unmyelinated fibers are fairly preserved, as shown under the electron microscope (B).

© 2013 American Academy of Neurology. Unauthorized reproduction of this article is prohibited.

Figure 4 Pedigree diagram and genetic studies

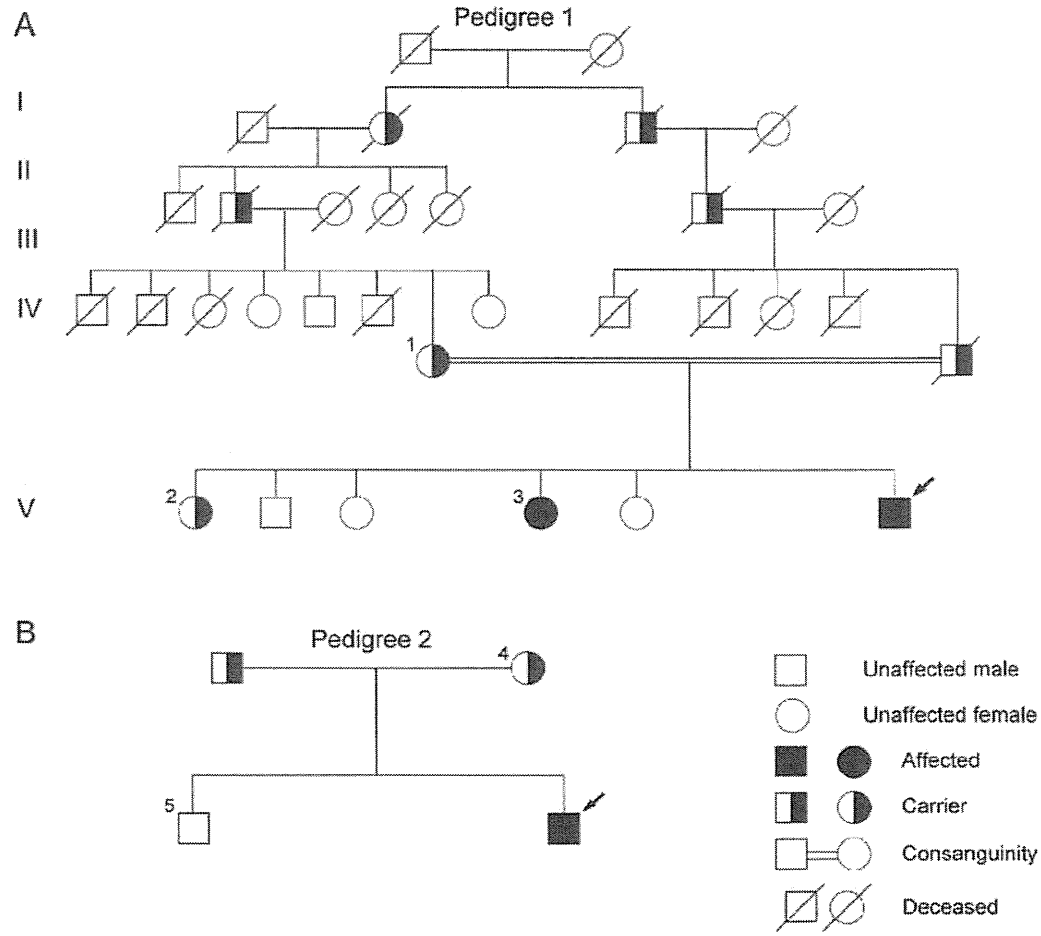

(A) Pedigree of patient 1. Patients 1 and 3 (V3) harbor the homozygous mutation, c.3993delGinsTT, whereas their mother (IV1) and 1 elder sister (V2) are heterozygous carriers. (B) Pedigree of patient 2. The same mutation, c.3993delGinsTT, can be observed in patient 2. His mother (4) exhibits the carrier genotype, and his elder brother (5) is normal. The black arrows (↙) indicate the proband. All the family members with available DNA samples are labeled with an Arabic numeral. (C) The c.3993delGinsTT mutation (↓) shifts the reading frame and generates a premature stop codon.

nor did we find it on the 1000 Genomes Web site, which catalogs human genetic variations using 2,500 patient samples, including 500 East Asian (100 Japanese) patient samples. DNA samples were then collected from 3 other family members of pedigree 1, and 2 members of pedigree 2. In patient 3, the same genotype was identified. In addition, asymptomatic carriers (mother and another elder sister of patient 1 and the mother of patient 2) and an unaffected member (brother of patient 2) were found (figure 4, A and B). This mutation changes the reading frame during the translation of the mRNA and generates a premature stop codon (figure 4C).

DISCUSSION Among the 16 disease-causing or related genes of HSAN, we identified a homozygous mutation in *SCN9A* from 2 Japanese families. We described 3 patients who presented with new clinical, in vivo electrophysiologic, and pathologic phenotypes.

SCN9A, which is located on chromosome 2q24.3, contains 26 coding exons.[32] It encodes $Na_v1.7$, which is the α-subunit of a tetrodotoxin-sensitive, voltage-gated sodium channel. $Na_v1.7$, composed of 4 domains, each with 6 transmembrane domains and 2 highly conserved pore-forming segments,[33] is preferentially expressed within the dorsal root ganglion and sympathetic ganglion neurons and their small-diameter peripheral

© 2013 American Academy of Neurology. Unauthorized reproduction of this article is prohibited.

axons.[34] It is crucial for the depolarizing phase of neuronal action potentials, and it seems to determine the excitability and repetitive firing properties of neurons.[35] Gain-of-function *SCN9A* mutations result in hyperexcitable nociceptive neurons and states, such as inherited erythromelalgia,[18] paroxysmal extreme pain disorder,[19] and small nerve fiber neuropathy,[20] whereas loss-of-function *SCN9A* mutations produce no sodium current and generate CIP.[22]

In our study, both families lived in the Kagoshima prefecture, which is located to the south of Kyushu Island, Japan, and both were unrelated to each other. Loss of pain and temperature perceptions began at different ages, appearing as early as birth in patient 2, in the second decade in patient 1, and in the third decade in patient 3. Their ages at the onset of symptoms were different from those reported for patients with CIP who had a congenital onset. Moreover, in these 3 patients, the area of their pain insensitivities was limited mainly within the distal part of the limbs, not the entire body, as is seen in patients with CIP. The sense of vibration and joint position were preserved in our patients. However, the predominant reduction in sweat production in our 3 patients, together with urination and defecation disorder, lacrimal secretion anomaly, and decreased number of fungiform papilla on the tongue in patient 2, suggested autonomic nervous system dysfunction. A recent study indicated that $Na_v1.7$ in sympathetic neurons also contributes to the sensation of neuropathic pain.[36] The severe rash and pigmentation may be due to a post-inflammatory hyperpigmentation, resulting from the disruption of autonomic innervation. Meanwhile, hyposmia/anosmia, which is a common feature in patients with CIP and loss-of-functional *SCN9A* mutation,[23,27,37] was also identified in our patients. Furthermore, in patient 2, hypogeusia was detected using a gustatory sensation test. Bone dysplasia, as an additional symptom in patient 2 (acetabular dysplasia, short humerus, and right hallux), had also been reported in a Dutch kindred.[38] The otorhinolaryngologist confirmed hearing loss, although at different levels, in patients 1 and 2, which has mainly been recorded in patients with HSAN type IE.[4-6] These findings definitely broaden the symptomatic heterogeneity of *SCN9A* mutations.

Although pain insensitivity was symmetrically detected in the distal portion of the limbs of the 2 index patients, nerve conduction studies only revealed asymmetric involvement of the extremities. These findings, except those of the peroneal nerve, were compatible with sensory-predominant axonal multiple mononeuropathy complicated by minimal demyelinating changes, rather than a polyneuropathy.

Interestingly, the pathologic features of the sural nerve in the 2 index cases also varied. Although decreases in the small and large myelinated fibers were observed among the fasciculi in patient 1, the extent was dramatically different, whereas the density of small and large myelinated fibers was fairly preserved in patient 2. These discoveries were consistent with the nerve conduction study findings, which suggested a mismatch between the distribution of affected fibers and the severity of the loss-of-pain sensations. In addition, especially in patient 1, both decreased large myelinated fibers and decreased SNAP/SCV indicated that the large myelinated fibers were affected, whereas cases with gain-of-function *SCN9A* mutations always present with small myelinated and unmyelinated fiber abnormalities.[20] The selective involvement of sensory nerves in these patients is inconsistent with the clinical features and may indicate that the dysfunction of the dorsal root ganglion is more predominant than that of the peripheral nerve. However, the mechanisms underlying the pathologic aberrations in the fasciculi or nerves, caused by the mutated $Na_v1.7$ in the dorsal root ganglion, require further research.

The homozygous mutation, c.3993delGinsTT, which is located in exon 22 of *SCN9A*, is expected to shift the reading frame from amino acid 1331 (p. leu1331phe) and generate a premature stop codon. This will induce an essential alteration in the fifth transmembrane segment of domain 3 in $Na_v1.7$ and eliminate the whole fourth domain. The nonsense-mediated messenger RNA decay mechanism will then be activated, which will induce loss of function of $Na_v1.7$ in nociceptive neurons. Together with the pedigree study that confirmed the cosegregation of the genotype and phenotype, this mutation was believed to be a pathogenic mutation.

In 3 patients from 2 Japanese families who experienced symptoms that were characterized by congenital or adolescence-onset loss of pain and temperature perception and autonomic nervous dysfunction accompanied by hyposmia, hearing loss, hypogeusia, bone dysplasia, and fractures, we identified a novel loss-of-function frameshift *SCN9A* mutation. We demonstrated that this was a new entity on the basis of clinical, in vivo electrophysiologic, and pathologic findings. We introduce this new entity as HSAN type IID, an allelic disorder with CIP, both of which result from loss-of-function mutations in *SCN9A*. Furthermore, on the basis of in vivo electrophysiologic and pathologic findings, we furthered the understanding of the mechanisms induced by the loss of function of $Na_v1.7$. We are able to summarize that a loss-of-function *SCN9A* mutation can produce heterogeneous phenotype, even harboring the same mutation.

AUTHOR CONTRIBUTIONS

Dr. Junhui Yuan: genetic study, analyses and interpretation of data, and drafting the manuscript. Dr. Eiji Matsuura: pathologic study of the sural nerve, analysis and interpretation of data, revising the manuscript. Dr. Yujiro Higuchi: acquisition and analysis of clinical data, revising the manuscript. Dr. Akihiro Hashiguchi: acquisition of clinical data

© 2013 American Academy of Neurology. Unauthorized reproduction of this article is prohibited.

and case selection. Dr. Tomonori Nakamura: nerve conduction study, analysis and interpretation of data. Dr. Satoshi Nozuma: acquisition of clinical data. Dr. Yusuke Sakiyama and Ms. Akiko Yoshimura: participated in genetic study. Dr. Shuji Izumo: analysis and interpretation of data. Dr. Hiroshi Takashima: study concept and design, interpretation of the data, revising the manuscript, study supervision, obtain funding.

ACKNOWLEDGMENT

The authors thank Ms. Y. Shirahama and A. Nishibeppu of our department for their excellent technical assistance. They also thank the Joint Research Laboratory, Kagoshima University Graduate School of Medical and Dental Sciences, for the use of their facilities.

STUDY FUNDING

Supported by the Intramural Research Grant (23-5) for Neurological and Psychiatric Disorders of NCNP; Research Committee for Neuropathy, Ataxic Disease and Applying Health and Technology of Ministry of Health, Welfare and Labour, Japan; and a research grant (23300201) from the Ministry of Health, Labour, and Welfare of Japan.

DISCLOSURE

Drs. Yuan, Matsuura, Higuchi, Hashiguchi, Nakamura, Nozuma, Sakiyama, and Ms. Yoshimura report no disclosures. Dr. Izumo received an honorarium for lecturing from Bayer Japan, funded by grants from Research Committee for HAM and neuroimmunological diseases of the Ministry of Health, Welfare and Labour of Japan. Dr. Takashima served on the scientific advisory board for Teijin, received a royalty from Athena diagnostics, was on the speakers' bureaus of Astellas, Bayer Group, Kyowa Hakko Kirin Pharma, Takeda Pharmaceutical Company Limited, Biogen Idec, Novartis, Dainippon Sumitomo Pharma, GlaxoSmithKline, Kowa Group, Pfizer Co., Mitsubishi Tanabe Pharma, and Eisai Co., is funded by grants from the Nervous and Mental Disorders and Research Committee for Ataxic Disease, Neuropathy, SMON, HAM, Chronic Pain, Applying Health and Technology of the Japanese Ministry of Health, Welfare and Labour, and received grants from Ministry of Education, Culture, Sports, Science, and Technology of Japan (grant 21591095). Go to Neurology.org for full disclosures.

Received November 2, 2012. Accepted in final form January 18, 2013.

REFERENCES

1. Dawkins JL, Hulme DJ, Brahmbhatt SB, Auer-Grumbach M, Nicholson GA. Mutations in SPTLC1, encoding serine palmitoyltransferase, long chain base subunit-1, cause hereditary sensory neuropathy type I. Nat Genet 2001;27:309–312.
2. Rotthier A, Auer-Grumbach M, Janssens K, et al. Mutations in the SPTLC2 subunit of serine palmitoyltransferase cause hereditary sensory and autonomic neuropathy type I. Am J Hum Genet 2010;87:513–522.
3. Guelly C, Zhu PP, Leonardis L, et al. Targeted high-throughput sequencing identifies mutations in atlastin-1 as a cause of hereditary sensory neuropathy type I. Am J Hum Genet 2011;88:99–105.
4. Wright A, Dyck PJ. Hereditary sensory neuropathy with sensorineural deafness and early-onset dementia. Neurology 1995;45:560–562.
5. Hojo K, Imamura T, Takanashi M, et al. Hereditary sensory neuropathy with deafness and dementia: a clinical and neuroimaging study. Eur J Neurol 1999;6:357–361.
6. Klein CJ, Botuyan MV, Wu Y, et al. Mutations in DNMT1 cause hereditary sensory neuropathy with dementia and hearing loss. Nat Genet 2011;43:595–600.
7. Lafreniere RG, MacDonald ML, Dube MP, et al. Identification of a novel gene (HSN2) causing hereditary sensory and autonomic neuropathy type II through the Study of Canadian Genetic Isolates. Am J Hum Genet 2004;74:1064–1073.
8. Coen K, Pareyson D, Auer-Grumbach M, et al. Novel mutations in the HSN2 gene causing hereditary sensory and autonomic neuropathy type II. Neurology 2006;66:748–751.
9. Kurth I, Pamminger T, Hennings JC, et al. Mutations in FAM134B, encoding a newly identified Golgi protein, cause severe sensory and autonomic neuropathy. Nat Genet 2009;41:1179–1181.
10. Rivière JB, Ramalingam S, Lavastre V, et al. KIF1A, an axonal transporter of synaptic vesicles, is mutated in hereditary sensory and autonomic neuropathy type 2. Am J Hum Genet 2011;89:219–230.
11. Slaugenhaupt SA, Blumenfeld A, Gill SP, et al. Tissue-specific expression of a splicing mutation in the IKBKAP gene causes familial dysautonomia. Am J Hum Genet 2001;68:598–605.
12. Anderson SL, Coli R, Daly IW, et al. Familial dysautonomia is caused by mutations of the IKAP gene. Am J Hum Genet 2001;68:753–758.
13. Axelrod FB, Hilz MJ. Inherited autonomic neuropathies. Semin Neurol 2003;23:381–390.
14. Mardy S, Miura Y, Endo F, et al. Congenital insensitivity to pain with anhidrosis: novel mutations in the TRKA (NTRK1) gene encoding a high-affinity receptor for nerve growth factor. Am J Hum Genet 1999;64:1570–1579.
15. Einarsdottir E, Carlsson A, Minde J, et al. A mutation in the nerve growth factor beta gene (NGFB) causes loss of pain perception. Hum Mol Genet 2004;13:799–805.
16. Carvalho OP, Thornton GK, Hertecant J, et al. A novel NGF mutation clarifies the molecular mechanism and extends the phenotypic spectrum of the HSAN5 neuropathy. J Med Genet 2011;48:131–135.
17. Edvardson S, Cinnamon Y, Jalas C, et al. Hereditary sensory autonomic neuropathy caused by a mutation in dystonin. Ann Neurol 2012;71:569–572.
18. Yang Y, Wang Y, Li S, et al. Mutations in SCN9A, encoding a sodium channel alpha subunit, in patients with primary erythermalgia. J Med Genet 2004;41:171–174.
19. Fertleman CR, Baker MD, Parker KA, et al. SCN9A mutations in paroxysmal extreme pain disorder: allelic variants underlie distinct channel defects and phenotypes. Neuron 2006;52:767–774.
20. Faber CG, Hoeijmakers JG, Ahn HS, et al. Gain of function Nav1.7 mutations in idiopathic small fiber neuropathy. Ann Neurol 2012;71:26–39.
21. Goldberg YP, Pimstone SN, Namdari R, et al. Human Mendelian pain disorders: a key to discovery and validation of novel analgesics. Clin Genet 2012;82:367–373.
22. Cox JJ, Reimann F, Nicholas AK, et al. An SCN9A channelopathy causes congenital inability to experience pain. Nature 2006;444:894–898.
23. Goldberg YP, MacFarlane J, MacDonald ML,, et al. Loss-of-function mutations in the Nav1.7 gene underlie congenital indifference to pain in multiple human populations. Clin Genet 2007;71:311–319.
24. Ahmad S, Dahllund L, Eriksson AB, et al. A stop codon mutation in SCN9A causes lack of pain sensation. Hum Mol Genet 2007;16:2114–2121.
25. Cox JJ, Sheynin J, Shorer Z, et al. Congenital insensitivity to pain: novel SCN9A missense and in-frame deletion mutations. Hum Mutat 2010;31:e1670–e1686.
26. Staud R, Price DD, Janicke D, et al. Two novel mutations of SCN9A (Nav1.7) are associated with partial congenital insensitivity to pain. Eur J Pain 2011;15:223–230.

© 2013 American Academy of Neurology. Unauthorized reproduction of this article is prohibited.

27. Nilsen KB, Nicholas AK, Woods CG, et al. Two novel SCN9A mutations causing insensitivity to pain. Pain 2009;143:155–158.
28. Schröder JM. Developmental and pathological changes at the node and paranode in human sural nerves. Microsc Res Tech 1996;34:422–435.
29. Dyck PJ, Giannini C, Lais A. Pathologic alterations of nerves. In: Dyck PJ, Thomas PK, Griffin JW, Low PA, Poduslo JF, editors. Peripheral Neuropathy, vol. 1, 3rd ed. Philadelphia: W.B. Saunders; 1993:514–595.
30. Milne I, Bayer M, Cardle L, et al. Tablet—next generation sequence assembly visualization. Bioinformatics 2010;26:401–402.
31. Okamoto Y, Higuchi I, Sakiyama Y, et al. A new mitochondria-related disease showing myopathy with episodic hypercreatine kinase-emia. Ann Neurol 2011;70:486–492.
32. Michiels JJ, te Morsche RH, Jansen JB, Drenth JP. Autosomal dominant erythermalgia associated with a novel mutation in the voltage-gated sodium channel alpha subunit Nav1.7. Arch Neurol 2005;62:1587–1590.
33. Klugbauer N, Lacinova L, Flockerzi V, Hofmann F. Structure and functional expression of a new member of the tetrodotoxin-sensitive voltage-activated sodium channel family from human neuroendocrine cells. EMBO J 1995;14:1084–1090.
34. Sangameswaran L, Fish LM, Koch BD, et al. A novel tetrodotoxin-sensitive, voltage-gated sodium channel expressed in rat and human dorsal root ganglia. J Biol Chem 1997;272:14805–14809.
35. Rush AM, Dib-Hajj SD, Liu S, Cummins TR, Black JA, Waxman SG. A single sodium channel mutation produces hyper- or hypoexcitability in different types of neurons. Proc Natl Acad Sci USA 2006;103:8245–8250.
36. Minett MS, Nassar MA, Clark AK, et al. Distinct Nav1.7-dependent pain sensations require different sets of sensory and sympathetic neurons. Nat Commun 2012;3:791.
37. Weiss J, Pyrski M, Jacobi E, et al. Loss-of-function mutations in sodium channel Nav1.7 cause anosmia. Nature 2011;472:186–190.
38. Hoeijmakers JG, Han C, Merkies IS, et al. Small nerve fibres, small hands and small feet: a new syndrome of pain, dysautonomia and acromesomelia in a kindred with a novel NaV1.7 mutation. Brain 2012;135:345–358.

Share Your Artistic Expressions in *Neurology* 'Visions'

AAN members are urged to submit medically or scientifically related artistic images, such as photographs, photomicrographs, and paintings, to the "Visions" section of *Neurology*®. These images are creative in nature, rather than the medically instructive images published in the Neuro*Images* section. The image or series of up to six images may be black and white or color and must fit into one published journal page. Accompanying description should be 100 words or less; the title should be a maximum of 96 characters including spaces and punctuation.

Learn more at *www.aan.com/view/Visions*, or upload a Visions submission at *submit.neurology.org*.

Save These Dates for AAN CME Opportunities!

Mark these dates on your calendar for exciting continuing education opportunities, where you can catch up on the latest neurology information.

Regional Conference

- October 25-27, 2013, Las Vegas, Nevada, Encore at Wynn Hotel

AAN Annual Meeting

- April 26-May 3, 2014, Philadelphia, Pennsylvania, Pennsylvania Convention Center

© 2013 American Academy of Neurology. Unauthorized reproduction of this article is prohibited.

Downloaded from jcp.bmj.com on August 29, 2013 - Published by group.bmj.com

Mitochondrial myopathy with autophagic vacuoles in patients with the m.8344A>G mutation

Jun-Hui Yuan, Yusuke Sakiyama, Itsuro Higuchi, Yukie Inamori, Yujiro Higuchi, Akihiro Hashiguchi, Keiko Higashi, Akiko Yoshimura, Hiroshi Takashima

▶ Additional material is published online only. To view please visit the journal online (http://dx.doi.org/10.1136/jclinpath-2012-201431).

Department of Neurology and Geriatrics, Kagoshima University, Graduate School of Medical and Dental Sciences, Kagoshima, Japan

Correspondence to
Dr Hiroshi Takashima, Department of Neurology and Geriatrics, Kagoshima University, Graduate School of Medical and Dental Sciences, 8-35-1 Sakuragaoka, Kagoshima City, Kagoshima 890-8520, Japan; thiroshi@m3.kufm.kagoshima-u.ac.jp

Received 28 December 2012
Accepted 11 March 2013 *
Published Online First 4 April 2013

ABSTRACT

Background and aims In mitochondrial myopathy, autophagy is presumed to play an important role in mitochondrial dysfunction. Rimmed vacuoles (RVs), a sign of autophagy, can be seen as a secondary phenomenon in muscle ragged-red fibres (RRFs), whereas the uncommon presentation is that some fibres contain RVs, but without any mitochondrial abnormalities. To investigate the pathogenesis beneath this pathological phenomenon.

Methods We reviewed 783 skeletal muscle specimens and selected five obtained from patients with suspected mitochondrial myopathy, characterised by clearly visible autophagic vacuoles in non-RRFs, besides the coexistence of RRFs and cytochrome oxidase-negative fibres. Immunohistochemical staining with LC-3, and electron microscopy studies were performed. Using resequencing microarray and a next-generation sequencing system, the mitochondrial DNA was screened for mutations and the heteroplasmic level was measured in skeletal muscle and blood.

Results Muscle fibres with RVs and RRFs, as well as some morphologically normal fibres, stained strongly for LC-3. Electron microscopy disclosed significant abnormal mitochondrial proliferation and existence of autophagic vacuoles. After mutation screening, m.8344A>G in the $tRNA^{Lys}$ gene was detected in two patients. The heteroplasmy of mutated G was 45.1% in skeletal muscle and 17.8% in blood in patient 1; patient 2 exhibited 80.3% mutated G in skeletal muscle and 25.2% in blood.

Conclusions These findings demonstrate a new pathological phenotype for the m.8344A>G mutation-related disease and also provide pathological evidence of a correlation between mitochondrial abnormalities and autophagy.

INTRODUCTION

Autophagy generally has a cytoprotective function, often preceding cellular apoptosis or necrosis. Cellular vacuoles that contain fragments of cell components are called autophagic vacuoles. Rimmed vacuoles (RVs) are characterised by small vacuoles lined by many red granules (the 'rim'), as observed by modified Gomori trichrome (mGT) staining and contain fragments of cellular components, including membrane whorls, as observed under electron microscopy. The RVs represent a type of autophagic vacuole and are non-disease-specific structures found in various myopathies, particularly in hereditary inclusion body myopathy, distal myopathy with RVs and inclusion body myositis (IBM).[1] Autophagy also contributes to the degradation of mitochondria (mitophagy),[2] and dysfunctional mitochondria may trigger the activation of the autophagic pathway.[3]

Ragged-red fibres (RRF) are characterised by the existence of subsarcolemmal zones of bright red or reddish blue material in mGT stain (figure 1), which result from the accumulation of abnormal mitochondria beneath the sarcolemma of muscle fibres. Histochemical demonstration of RRFs and cytochrome c oxidase-negative fibres on muscle biopsy is considered to be the hallmark of a mitochondrial myopathy.[4] In our experience, RVs can be seen in the RRFs, as a secondary change of abnormal mitochondrial accumulation. On the other hand, it has been shown that frequent RRFs can be found in patients with IBM and may reflect an age-related decline in muscle mitochondrial oxidative metabolism.[5] Nevertheless, in five Japanese patients with suspected mitochondrial myopathy, we found that besides the prominent feature of RRFs, noticeable RVs appeared in the non-RRFs—an unexpected phenomenon.

m.8344A>G mutation in the $tRNA^{Lys}$ gene can result in a myoclonic epilepsy with RRF (MERRF syndrome) and is present in over 80% of affected subjects. Genetic analysis showed an m.8344A>G mutation in two of our patients. Typical MERRF syndrome is characterised by myoclonic epilepsy, cerebellar ataxia and RRFs in skeletal muscle tissue.[6] However, in this study, the phenotypes of the two patients with the m.8344A>G mutation were atypical; they had proximal muscle weakness and external ophthalmoplegia or preferential facioscapulohumeral muscle involvement.

We demonstrate a new pathological phenotype for the m.8344A>G mutation. These findings suggest a distinct pathogenesis between mitochondrial abnormalities and autophagy. The isolated autophagic vacuoles may also be associated with the atypical clinical phenotype of patients with an m.8344A>G mutation.

MATERIALS AND METHODS

Subjects

We examined 783 skeletal muscle specimens obtained from patients who were referred to our department between 2001 and 2011. Twenty-seven patients with definite coexistence of RRFs and RVs were selected, and then those with IBM (10 patients), dermatomyositis (three patients), polymyositis (one patient), amyotrophic lateral sclerosis (two patients), myotonic dystrophy (one patient) and non-specific myopathy (five patients) were excluded. Based on the clinical features, marked RRFs and cytochrome c oxidase-negative fibres in pathology, five Japanese patients with suspected

To cite: Yuan J-H, Sakiyama Y, Higuchi I, *et al*. *J Clin Pathol* 2013;66:659–664.

Downloaded from jcp.bmj.com on August 29, 2013 - Published by group.bmj.com

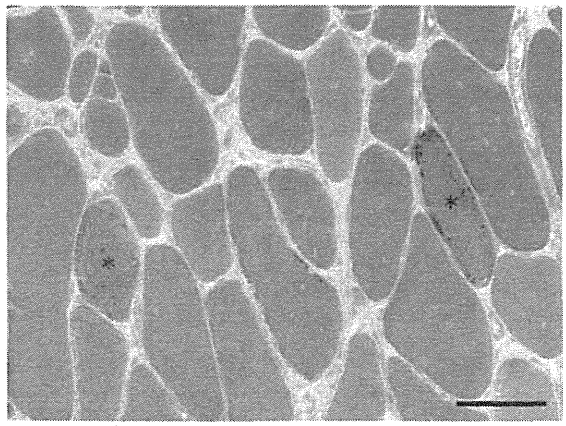

Figure 1 Modified Gomori trichrome staining of muscle ragged-red fibres (RRFs). RRFs are indicated by (*). Bar=100 μm. Access the article online to view this figure in colour.

mitochondrial myopathy were chosen for this study. Of these patients, only two who had the m.8344A>G mutation are described herein. No pathogenic mutation was detected in mtDNA from the other three patients. In addition, between 2001 and 2011, we identified the m.8344A>G mutation in blood from six of 169 patients with suspected mitochondrial disorders. Three of these patients underwent a muscle biopsy: two patients comprised the patients previously selected and the other exhibited a typical MERRF syndrome. However, because no definite RVs were seen in skeletal muscle, this last patient was excluded from the study.

All the diagnoses were made by experienced neurologists and pathologists based on clinical and laboratory examinations, electrobiological studies and skeletal muscle pathology.

Patient 1

A 51-year-old man with no family history of myopathy complained of general fatigue which he had had for 15 years. He began to experience muscle weakness from 36 years of age. This weakness gradually worsened, and by the age of 40 years he had difficulty in walking. Over the following 3 years, the symptoms progressed until he was incapable of lifting any substantial weight. Physical examination showed moderate muscle weakness in the facial, cervical and proximal muscles. His eye movements were also restricted in the superoinferior direction and he had difficulty hearing high-pitched voices. His serum creatine kinase level was raised at 1378 U/l (normal range 45–163 U/l).

Patient 2

A 54-year-old man reported a 24-year history of muscle weakness; there was no family history of any such difficulty. At 30 years of age, he experienced difficulty in lifting his arms and his cervical muscles gradually became affected. He occasionally tumbled down staircases; one fall required admission to hospital for a subarachnoid haemorrhage. Physical examination at the time of study enrolment showed marked weakness and wasting of the shoulder girdle muscles, without scapular winging. The facial muscles, intrinsic muscles of the hand and thigh muscles were also found to be atrophied. The extraocular muscles and the cranial nerves were normal and no other abnormalities were detected. His serum creatine kinase level was 46 U/l. CT indicated myoatrophy in his arms.

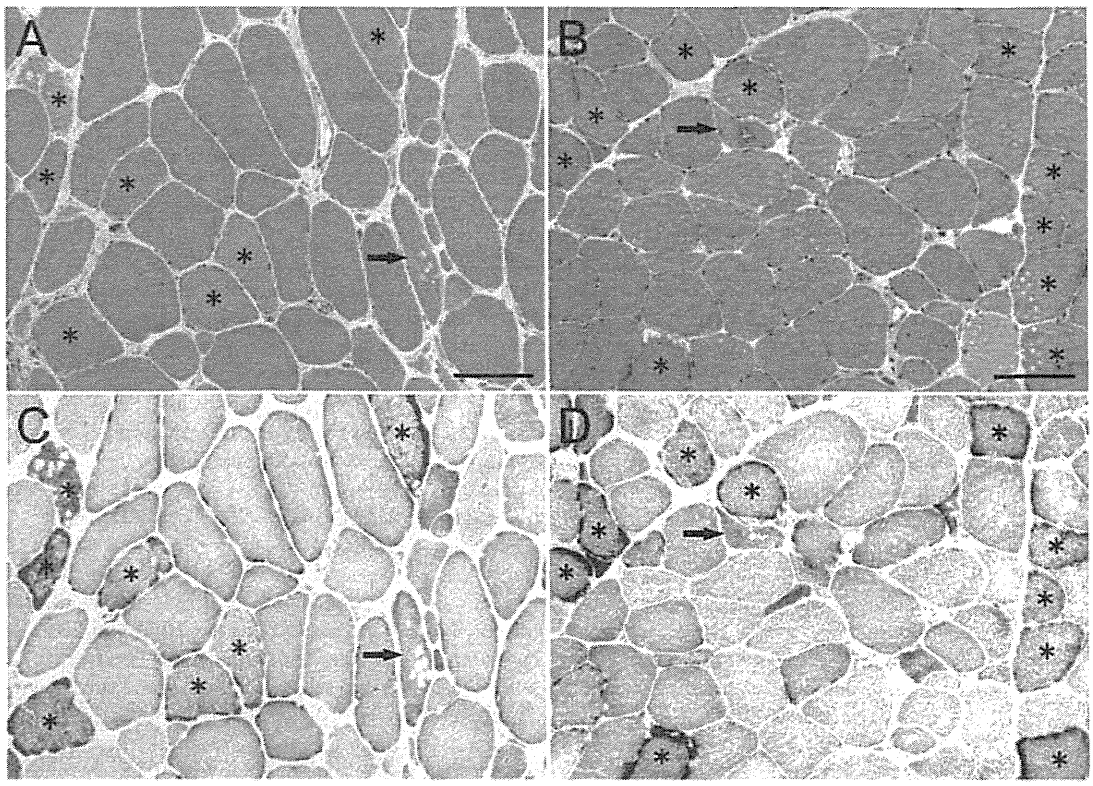

Figure 2 Histochemical staining of muscle ragged-red fibres (RRFs) and isolated rimmed vacuoles in patient 1 (A and C) and patient 2 (B and D). Haematoxylin and eosin (A and B) and succinate dehydrogenase (C and D) staining shows numerous RRFs (*), coexisting with non-RRFs containing rimmed vacuoles (arrow). Bar=100 μm. Access the article online to view this figure in colour.